AIAA 2004-4182

Incorporation of Nonlinear Capabilities in the Standard Stability Prediction Program

G. A. Flandro and J. Majdalani
Advanced Theoretical Research Center
University of Tennessee Space Institute
Tullahoma, TN 37388

J. C. French
Software and Engineering Associates, Inc.
Carson City, NV 89701

40th AIAA/ASME/SAE/ASEE Joint Propulsion Conference and Exhibit
11–14 July 2004
Fort Lauderdale, FL

40th AIAA/ASME/SAE/ASEE Joint Propulsion Conference and Exhibit
11-14 July 2004, Fort Lauderdale, Florida

AIAA 2004-4182

Incorporation of Nonlinear Capabilities in the Standard Stability Prediction Program

Gary A. Flandro* and Joseph Majdalani†
University of Tennessee Space Institute, Tullahoma, TN 37388
and
Jonathan C. French‡
Software and Engineering Associates, Inc., Carson City, NV 89701

Predictive algorithms now in general use cannot characterize high-amplitude pressure oscillations that are frequently observed in solid propellant rocket motor combustion chambers. In fact, programs such as the Standard Stability Prediction (SSP) code are based on a linear theory, which has serious shortcomings. Therefore, it is necessary to address both correction of the flawed linear theory and incorporation of models to allow prediction of important nonlinear effects. These include: 1) *limit cycle behavior* in which the pressure fluctuations may dwell for a considerable period of time near their peak amplitude, 2) elevated mean chamber pressure (*DC shift*), and 3) a *triggering* amplitude above which pulsing may cause an apparently stable system to transition to violent oscillations. Culick's well-established nonlinear model provides useful guidance in dealing with the system limit cycle transition. It is demonstrated in this paper that his calculations represent the classical steepening mechanism by which the wave system evolves from an initial set of standing acoustic modes into a shock-like, traveling, steep-fronted wave. However, a very important missing element is the ability to predict the accompanying mean pressure shift; clearly, the program user requires information regarding the maximum chamber pressure that might be experienced during operation of the motor, as well as the peak amplitudes reached by the pressure oscillations. Recent theoretical work has resulted in a firm foundation upon which to build the required predictive capabilities. These are described in detail, and it is demonstrated that the new theory yields results that are in excellent agreement with experimental data.

Nomenclature

$\bar{a}$	Mean speed of sound
e	Oscillatory energy density
$\bar{E}$	Time-averaged oscillatory system energy
E_m^2	Normalization constant for mode m
k_m	Wave number for axial mode m
L	Chamber length
m	Mode number
$\bar{M}$	Reference Mach number in chamber
$\boldsymbol{n}$	Outward pointing unit normal vector
p	Oscillatory Pressure
$\bar{P}$	Mean chamber pressure
r	Radial position
R	Chamber radius
t	Time
$\boldsymbol{u}$	Oscillatory velocity vector
z	Axial position
Greek	
α	Growth rate
δ	Inverse square root of the acoustic Reynolds number, $\sqrt{\nu / a_0 R}$
γ	Ratio of specific heats
ε	Wave amplitude
ν	Kinematic viscosity, μ / ρ
ρ	Density

*Boling Chair Professor, Mechanical and Aerospace Engineering. Associate Fellow AIAA.
†Jack D. Whitfield Professor of High Speed Flows, Mechanical and Aerospace Engineering. Member AIAA.
‡ Senior Research Engineer. Member AIAA.

ω	Unsteady vorticity amplitude
Ω	Mean vorticity amplitude

Subscripts

b	Combustion zone
m	Mode number

Superscripts

*	Dimensional quantity
~	Vortical (rotational) part
^	Acoustic (irrotational) part
(r), (i)	Real and imaginary parts
(1)	Indicates first-order accuracy

I. Introduction

COMBUSTION instability in solid propellant rocket motors is frequently associated with sound waves, since measured frequencies are closely approximated by simple acoustic theory. For this reason, analytical work aimed at providing physical insight into the phenomenon is, quite naturally, founded upon the notion of perturbed acoustic waves.[1-10] All predictive codes are built upon these concepts.[2-4,7-20] This includes the SSP (Standard Stability Prediction) program now used almost universally in treating instability problems. Most such predictive algorithms represent only the *linear* features of the instability, and provide no information regarding important nonlinear features of great practical significance.

A typical SSP calculation yields only a set of growth rates based on the underlying linear theory. Usually these are net growth rates for each acoustic mode and burn time selected by the analyst. If, for example, all of these are found to be negative, then the system is deemed to be stable. If one (or more) is positive, the user interprets this to mean that there is a potential instability problem. That is, there may be a *tendency* for the motor to oscillate. No information is forthcoming regarding what amplitude such oscillations are likely to attain, or whether or not the system is susceptible to triggered instability initiated by random or deliberate pulsing.

The *limit cycle*, or peak amplitude reached by the oscillations, is obviously an important quantity since it reflects the vibration environment produced by the instability. Attempts have been made to understand this limiting behavior of the wave system by including nonlinear corrections that extend the linear acoustic instability theories.[5,6,8,21-26] These efforts have been useful in demonstrating certain essential physical phenomena, such as the natural steepening mechanism that causes initially low-amplitude acoustic waves to transition into shock-like structures.[6,21,23,24,27-29] The central role played by shock waves in nonlinear longitudinal mode combustion instability has also been convincingly demonstrated experimentally.[30]

More importantly, no information is provided regarding the much dreaded *DC shift*, or mean pressure excursion that often accompanies finite-amplitude oscillations. It is curious that although the DC shift was, historically, the first observed sign of combustion instability, its true origin and its exact nature have never been successfully established.[14,31,32] Therefore, considerable attention is devoted in this paper to rectifying this situation. In particular we seek to understand in detail its obvious connection to the oscillatory gas motions and the controlling factors in terms of chamber geometry and physical parameters.

In this paper we apply a new set of analytical tools that have evolved from many decades of struggle with the solid propellant rocket combustion instability problem. Recent work by the present authors has led to considerable progress in the development and refinement of predictive capability. To be useful, such tools must go far beyond the usual linear growth rate calculations. To be complete, the analysis must account for:

- Steep-fronted, shocked pressure waves,
- effects of rotational flow interactions,
- combustion coupling including: unsteady distributed energy release, detonation wave phenomena, and interactions with the propellant combustion processes, and
- mean pressure shift and its coupling with the oscillatory flow field.

In order to achieve understanding of these nonlinear phenomena, it is vitally important to start with a valid linear model. Unfortunately, the linear theory on which the SSP is based has serious flaws. As we shall demonstrate, despite many claims to the contrary, the code does not adequately predict even the linear stability features for a given motor configuration.

Over the years, analysts have devised corrective terms in attempts to yield better agreement with experiments. Some of these have been based on sound theoretical ground; others are little more than speculation. Clearly, if the SSP user is armed with enough variable parameters, he can fit any data set and thereby convince himself that he has adequately predicted the motor behavior. When the same model incorrectly portrays another system configuration, the failure is often blamed on inadequate knowledge of key system parameters such as the propellant admittance or response function.

To make progress, we must begin by providing a complete and correct linear representation of combustion instability. Then upon this platform we can erect nonlinear models to extend the linear results into the finite-amplitude regime. We demonstrate these steps in this paper.

The third author is currently incorporating the resulting computational modules in the SSP code. The validity of the basic analyses on which these are based are tested in this paper by comparing predicted motor behavior to experimental data from several previous studies.[14,31-36] We also demonstrate how the improved theoretical understanding leads to new methods for measuring the vital propellant response function.

II. Improving Linear Stability Theory

It would be futile to mount an attack on the nonlinear combustion instability problem without a valid linear model upon which to build. That is, if we cannot accurately represent the gas motions at very low amplitudes near the stability boundary, then there is scant hope of resolving their behavior as they grow to finite amplitude. Let us first examine some typical experimental data to test current SSP capabilities.

A. Blomshield's Tactical Motor Tests

An extensive data set employing full scale pulsed tactical rockets was secured in a series of highly instrumented firings.[34] These exhibited the classical attributes of nonlinear combustion instability. Data reduction was accomplished by means of the linear SSP algorithm. Figure 1 shows the resulting correlation of the measured growth rates to SSP predictions. Data points on the left represent decaying pulses; those on the right were growing pulses.

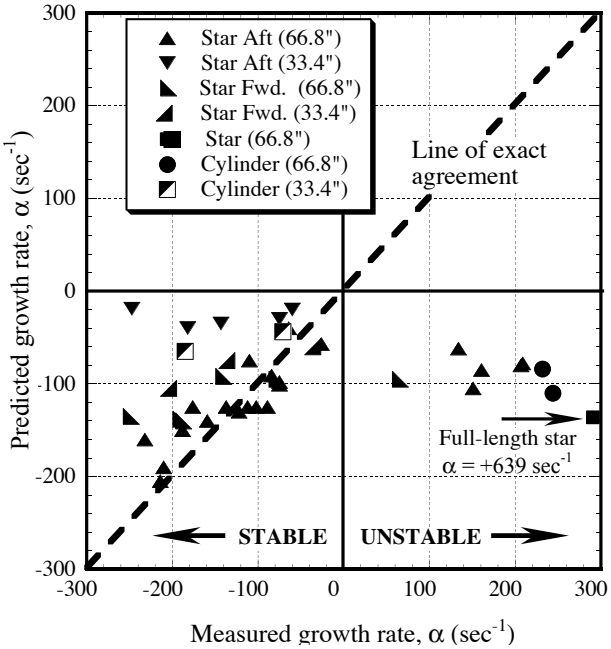

Fig. 1 Measured vs. theoretical growth rates.[34]

Note that exact agreement between theory and experimental data is indicated when the data point lies on the diagonal line. It is distressing that instability was never predicted by SSP; all data points in Fig. 1 fall on the negative side in terms of predicted growth rate. When data from firings that exhibited decaying pulses were compared to the SSP predictions, it was felt that acceptable agreement had been demonstrated. The authors wrote "… in all cases the trends in measured instability were confirmed by the Standard Stability Program." However, the growing pulses indicated extremely poor agreement! The reason for this discrepancy seems clear: decaying pulses correspond to tests where negative net growth rates prevail. Therefore, as oscillations decay, they tend to approach amplitudes sufficiently small to behave in a nearly linear fashion. On the other hand, growing pulses rapidly reach amplitudes dominated by nonlinearity. It must be pointed out that, even for decaying pulses, there is strong evidence that nonlinear effects control the gas motions. Predictive capability of SSP indicated on the left side of Fig. 1 is not acceptable.

Of even greater concern is that the linear theory does not predict the positive growth rates when pulsing leads to growing disturbances; these are correctly characterized as *triggered* instabilities. However, there is a subtle implication that there must be some basic difference between motors with growing pulses and those that decay. We will presently show that this is simply related to conditions leading to positive linear growth rates. That is, these motors are made susceptible to pulsing because (despite the predictions of stability from the SSP) they must be linearly unstable systems. The important message here is that there is something amiss with SSP.

The Blomshield data displays all of the attributes of nonlinear behavior that are discussed in the Introduction. The spectra corresponding to growing oscillations were rich in harmonics indicating a steepened wave structure. The DC pressure shift was closely correlated with the growth in the oscillations, and a distinct limit cycle was observed. Clearly, if such nonlinear instability is to be understood, a prerequisite must be a valid linear approximation on which to build. This theme guides the work described herein.

For emphasis, *all* motor configurations in this test series were predicted to be stable as indicated by all points in Fig. 4 lying in the lower half of the graph. Therefore, it is the opinion of the authors that linear theory fails in accounting for Blomshield's measurements. Thus, we are challenged to identify the reasons for the serious lack of agreement between the linear theory and experimental data for cases in Fig. 4 where linear theory should be applicable.

B. Perturbed Acoustic Wave Equation Models

Current understanding of the instability problem from the linear point of view has evolved over many decades and is the work of many outstanding analysts. The linear theory has been constantly modified by incorporating experimental knowledge – the scientific method in action! However, the model upon which the current version of SSP is based has inherent limitations that result from assumptions used in its formulation. We now briefly review each of these and seek ways to avoid the related pitfalls.

As already pointed out, the close correspondence between measured wave oscillation frequency and the acoustic normal mode frequencies of the combustion chamber leads irresistibly to the notion that the observed oscillations are acoustic pressure waves. Then it is natural to use a stability model based on the acoustic wave equation with perturbation terms to account for the mean flow, combustion at propellant surfaces, viscous losses, and two-phase flow effects (particle damping). Culick and his co-workers have honed this scheme to a fine edge; it forms the basic foundation for the SSP.[2-8,11,12,19-22,27,28,37-42] Culick also uses this basic structure for nonlinear stability theory by retaining second order coupling terms.

There are several concerns with the acoustic wave model. The first of these is that such waves do not satisfy correct boundary conditions at the chamber walls, especially at burning surfaces. Culick encountered this difficulty in his one-dimensional (1D) stability calculations.[3,11] In that analysis he correctly forced the unsteady and unsteady flow to enter the chamber in the normal (perpendicular to the propellant surface) direction. Although allowed in the 1D formulation, this step cannot be taken in the three-dimensional problem without regard for the actual physical nature of the acoustic boundary layer. His one-D model then yielded new stability terms that did not appear in the 3D analysis. The most important of these was the *flow turning* effect, which Culick theorized must represent "non-elastic" losses incurred as gas particles entering normally are forced into the axial direction of the primary wave motion. The resulting damping correction factor proved in most cases to be of the same order of magnitude as the driving contributions from pressure coupling, the main energy source for the oscillations.

C. The Flow Turning Energy Loss

Flow turning was incorporated from the outset in the SSP and is frequently used for both 1D and 3D computations. Its presence is the principal reason for overly stable SSP predictions that may give comfort to rocket industry executives, but leads to incorrect predictions in many applications.

Users of the SSP code have the option of switching flow turning on or off. It has been often noted that better predictions result when it is not activated. On the other hand, some analysts have felt that better agreement results by including the flow turning correction.

A rational three-dimensional model for flow turning was devised by the present authors, and its true origin was discovered in the creation of unsteady vorticity at propellant when gas motions are parallel to the boundary.[43-47] However, in this process, additional stability corrections related to vorticity production were discovered. One of these was found to effectively cancel the flow turning effect. This was originally called the *rotational flow correction* for want of a better name.[44-46]

D. The Boundary Layer Pumping Effect

Since the rotational flow correction, or *boundary layer pumping* is a destabilizing influence equal in rank to the flow turning damping, its origin and significance must be understood. We will do so without a lengthy theoretical exposition. It is only necessary to recall well-established ideas from fundamental boundary layer theory.

Consider a flat plate starting impulsively and then moving at constant speed into a fluid at rest as illustrated in Fig. 2a. A viscous boundary layer is formed in order that the no-slip constraint is satisfied. From the point of view of an observer moving with the plate, the growing boundary layer induces a flow normal to the surface because of the displacement effect as shown in Fig 2b. This normal velocity correction is equivalent to a source distribution on the plate. In other words, the mass defect caused by the boundary layer requires that there be a normal induced velocity to account for the mass entering the boundary layer parallel to the surface.

The same mass conservation effect explains the origin of the boundary layer pumping mechanism.

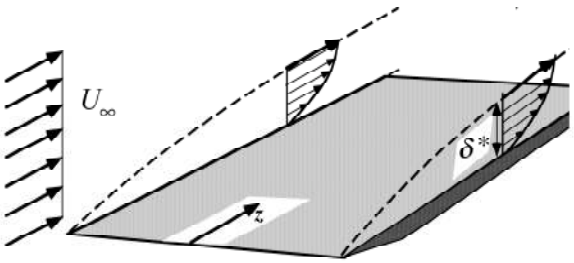

a) Boundary layer effect on external flow is equivalent to a source distribution on the surface

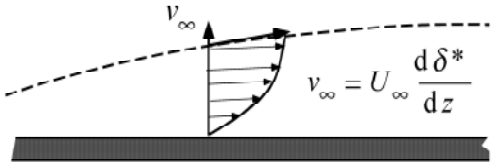

b) Induced velocity normal to surface due to the displacement effect

Fig. 2 The boundary layer displacement effect.

The unsteady flow near the burning surface (when the gas motions are parallel to the surface) is controlled by both the unsteady burning of the propellant in response to the pressure fluctuations (pressure coupling) and by unsteady boundary layer displacement. To visualize the latter, imagine that the plate in Fig. 2 undergoes oscillation parallel to the surface. This is the familiar Stokes' second problem. An unsteady boundary layer is produced and with it an unsteady normal velocity fluctuation analogous to the steady one shown in Fig. 2. This is the origin of the rotational flow correction. In order that mass conservation is satisfied, this correction to the normal velocity created in the pressure coupling process must be accounted for. Flandro[44-46,48] found that the effect on the linear system growth rate is given in dimensionless form by

$$\alpha_5 = \frac{1}{2E_m^2} \iint_{S_{b\|}} M_b \left(p'_m\right)^2 \mathrm{d}S \qquad (1)$$

where m is the mode integer. This growth rate contribution arises only at burning surfaces that experience a parallel acoustic velocity component; hence the notation on the surface integral. The subscript, 5, pertains to a numbering system used in Ref. (46) to account for the various linear growth rate contributions. It was perhaps fortuitous that this term when evaluated for a full length cylindrical motor yields a growth contribution that cancels the corresponding flow turning correction. However, as we shall demonstrate, the flow turning is exactly cancelled by other terms that have only recently been discovered. Their absence in the earlier analyses was largely the result of applying the perturbed acoustic wave formulation. In order to achieve the correct result, it is necessary to account for all unsteady energy pathways. We will return to this matter in a later subsection.

In any event, the destabilizing mechanism described here both in a simple physical analogy and in a complete theoretical analysis must be incorporated in the linear stability assessment whenever wave motions parallel to a burning surface are present.

E. Velocity Coupling

Another corrective mechanism was introduced by McClure and his coworkers[49] intended to account for the effects of gas motions parallel to the burning surface. These rather elaborate analyses were quite naturally configured as unsteady extensions of the steady state combustion properties of solid propellants. The ideas of acoustic erosivity, velocity rectification, flow reversal, and threshold amplitude were thus introduced into a theoretical environment already cluttered with ill-defined concepts. The unfortunate aspect of all of these *velocity coupling* ideas is that they assumed that the parallel fluctuating gas velocity component acts directly at the propellant surface leading to the concept of the "cross-flow velocity" and associated paraphernalia. The importance of the no-slip condition was not recognized, and the literature is replete with discussions attempting to sort out which part must be treated as nonlinear and how linear velocity coupling can arise. There has never been consensus on these issues mainly because of the questionable assumptions and lack of experimental evidence, other than the usual nonlinear instability attributes which we will show in this paper are readily understood without the need for and ill-defined velocity coupling mechanism.

Eventually, an *ad hoc* linear velocity coupling model was adopted and it is still available in the SSP code. In order to use this growth rate term it is necessary to specify a *velocity coupling response function* that, by analogy with pressure coupling, must come from experimental measurements. No successful measurements were ever demonstrated, so the user is forced to guess at an appropriate value. Since there is so much uncertainty regarding the validity of velocity coupling, the wise analyst always picks a low value for the response function. This leads to a growth rate that is usually an unimportant contribution to the net system growth. On the other hand, one can always resort to adjusting values of the velocity coupling in an attempt to correct discrepancies between observed instabilities and the SSP predictions. This is not an acceptable approach. In order to be a truly predictive, the algorithm must be based only on mechanisms with a sound physical basis and which are supported by calculated or experimentally determined parameters.

More recent work (cf. Ref. 44) has accounted for the correct boundary conditions; a rational model for the effects of parallel wave incidence has emerged.

The authors suggest (with some trepidation) that the growth term shown in Eq. (1) be renamed as the linear velocity coupling. Its origin is clearly the interaction of the parallel gas motions with the burning surface. Although it does not modify the unsteady combustion processes that are controlled by the pressure fluctuations, it does indeed represent an additional stability mechanism of considerable importance. No response function of uncertain origin is needed in its evaluation.

F. Other Linear Stability Effects

There are several other contributions to the gain/loss balance that sets the net growth rate.[46] For the most part these are based on very sound theory, and at least at present there does not seem to be a major need for revisions. Thus, the usual particle damping analysis so elegantly worked out by Culick,[8] and the effects of nozzle damping, are assumed to be adequately handled in the present version of SSP.

G. Applying the Energy Method

In order to achieve a reliable linear stability algorithm, one must obviously account for all energy gains and losses. We have pointed out the pitfalls of attempting to do this in the context of the perturbed acoustic wave equation method. It is clear that the gas motions that we must model are only partly acoustic in nature. The acoustic assumption implies that rotational flow effects and nonisentropic effects are of secondary importance. We have already demonstrated that this is not the case.

To rectify this situation, it is necessary to reformulate the problem and to carefully account for every possible energy pathway. Full details of the resulting analytical technique are given in a companion paper.[50] We will simply state the results here and point out the improvements that have been made.

If the full energy balance is used in the problem formulation, it is possible to carry out both the linear and nonlinear calculations in one step. Both linear and nonlinear energy pathways are thus illuminated. To illustrate this, we will now briefly introduce one or two intermediate steps. The starting point is the conservation form of the energy equation

$$\frac{\mathrm{D}}{\mathrm{D}t}\left[\rho\left(e+\tfrac{1}{2}\boldsymbol{u}\cdot\boldsymbol{u}\right)\right]=\left\{\begin{array}{l}\dfrac{\delta^2}{\left(\gamma-1\right)Pr}\nabla^2 T-\dfrac{1}{\gamma}\nabla\cdot\left(p\boldsymbol{u}\right)\\ +\rho\boldsymbol{u}\cdot\left(\boldsymbol{u}\times\boldsymbol{\omega}\right)-\dot{Q}+\boldsymbol{u}\cdot\boldsymbol{F}\\ +\delta^2\left[\boldsymbol{\omega}\cdot\boldsymbol{\omega}-\boldsymbol{u}\cdot\nabla\times\boldsymbol{\omega}\right]\\ +\delta_d^2\left[\left(\nabla\cdot\boldsymbol{u}\right)^2+\boldsymbol{u}\cdot\nabla\left(\nabla\cdot\boldsymbol{u}\right)\right]\end{array}\right\} \quad (2)$$

where provision has been made for both dissipative and non-dissipative energy changes. If it is assumed that both the steady and unsteady flowfields are known to first-order accuracy, then the standard separation of non-oscillatory and fluctuating variables leads to an expression for the rate of change of the amplitude of the wave system of the form

$$\frac{\mathrm{d}\varepsilon}{\mathrm{d}t}=\alpha^{(1)}\varepsilon+\alpha^{(2)}\varepsilon^2+\alpha^{(3)}\varepsilon^3+\cdots \quad (3)$$

where the first coefficient is the required net linear growth rate.

In working with Eq. (2) one finds the origin of the *flow turning* and other rotational flow effects in the first set of terms involving the vorticity on the right-hand side. In the process of evaluating the system stability, we find that these terms lead to a stability contribution of the form

$$\alpha_4^{(1)}=\frac{\bar{M}_b\bar{P}}{2E^2}\iiint_V\left(\boldsymbol{U}\cdot\left\langle\boldsymbol{u}'\times\boldsymbol{\omega}'\right\rangle+\left\langle\boldsymbol{u}'\cdot\boldsymbol{U}\times\boldsymbol{\omega}'\right\rangle\right)\mathrm{d}V \quad (4)$$

where the notation again corresponds to that introduced in Ref. 46. The first term in this expression was missing in the stability assessment given in that report because a complete energy balance was not used. The method employed in that work was based, in effect, on the acoustic wave equation approach; therefore, only a partial accounting of rotational flow corrections was made. Furthermore, the results were based on the isentropic assumptions, which is another limitation we avoid in the new computations.

Flow turning was first identified by Culick[3,11] in his one-dimensional calculations as a result of forcing satisfaction the no-slip condition (which could not be accomplished in his three-dimensional model because of the irrotational flow assumption). Flandro[44-47] later showed that the actual source of the flow turning was the irrotational part of the second term in Eq. (4). None of the earlier stability calculations incorporated all of the rotational terms included in Eq. (4). These appear because we have now used a complete energy balance equation. When *all* of the terms are properly accounted for, then application of the familiar *scalar triple product* identity

$$\boldsymbol{A}\cdot\left(\boldsymbol{B}\times\boldsymbol{C}\right)=\boldsymbol{B}\cdot\left(\boldsymbol{C}\times\boldsymbol{A}\right) \quad (5)$$

leads to

$$\begin{aligned}&\boldsymbol{U}\cdot\left\langle\boldsymbol{u}'\times\boldsymbol{\omega}'\right\rangle+\left\langle\boldsymbol{u}'\cdot\boldsymbol{U}\times\boldsymbol{\omega}'\right\rangle=\\&\quad=\left\langle-\boldsymbol{u}'\cdot\boldsymbol{U}\times\boldsymbol{\omega}'\right\rangle+\left\langle\boldsymbol{u}'\cdot\boldsymbol{U}\times\boldsymbol{\omega}'\right\rangle=0\end{aligned} \quad (6)$$

Flow turning has now utterly disappeared, having been cancelled exactly. This result agrees with much experimental evidence and with other key analyses.[51,52]

This correction to the linear growth rate leads to major improvement in agreement with experimental data. The lesson here is that only by accounting for *all* unsteady energy gains and losses can a correct linear stability theory be achieved. Other terms in Eq. (2) once thought to have important stability implications do not appear when the integrals are carefully evaluated.

One then finds that the linear stability of the system is controlled by

$$\alpha^{(1)}=\left\{\begin{array}{l}\dfrac{1}{2\gamma^2E^2}\iint_{S_b}\bar{M}_b\left(A_b^{(r)}+\dfrac{1}{\gamma\bar{P}}\right)\left\langle\left(p'\right)^2\right\rangle\mathrm{d}S\\ \qquad\text{Pressure Coupling}\\ -\dfrac{1}{2\gamma^2E^2}\iint_{S_N}\bar{M}_N\left(A_N^{(r)}+\dfrac{1}{\gamma\bar{P}}\right)\left\langle\left(p'\right)^2\right\rangle\mathrm{d}S\\ \qquad\text{Nozzle Damping}\\ +\quad\dfrac{1}{2\gamma^2E^2}\iint_{S_{b\|}}\bar{M}_b\left\langle\left(p'\right)^2\right\rangle\mathrm{d}S\\ \qquad\text{Velocity Coupling (Rotational Flow Correction)}\\ +\ldots\end{array}\right\} \quad (7)$$

where particle damping, distributed combustion, and viscous damping effects are not shown. Although the first two terms are the familiar pressure coupling and nozzle damping effects, some important changes have appeared. Of great significance is the presence of the quasi-steady mean pressure in the linear growth rate expression. This is the result of allowing the mean properties to change slowly (on the scale of the fluctuating properties) with time. This is a major modification and is coupled with the calculation of the important mean pressure excursion (DC shift) that we will address shortly. Also, as a result of eliminating the isentropic flow assumption there are new appearances of the specific heat ratio, γ, and there are corresponding changes in the system reference energy. We find that

$$E^2 = \iiint_V \left\langle \frac{1}{\gamma \bar{P}} \left(\frac{p'}{\gamma} \right)^2 + \frac{1}{2} \bar{P} \boldsymbol{u}' \cdot \boldsymbol{u}' \right\rangle \mathrm{d}V \qquad (8)$$

where the kinetic energy term must now be based on the full acoustic/shear wave model. This results in a kinetic energy contribution which is approximately 25% larger than for the acoustic model alone.[46] Again, notice the presence of the quasi-steady mean pressure in this expression. At the outset we expect significant coupling between changes in the wave amplitude and in the chamber pressure as we seek to model the full system time history.

The corrections introduced in the linear model and summarized in Eq. (7), partially account for the poor agreement between theory and experiment portrayed in Fig. 1. It is plain that major nonlinear interactions are reflected in the measurements. Thus, to make further progress, we must seek to introduce nonlinear corrections that can be used effectively in the SSP computational suite.

III. Nonlinear Instability Algorithm

In this section we briefly discuss what is needed from the theoretical standpoint to provide a useful analytical framework for combustion instability. It is necessary to accommodate the features we have identified as key elements in a correct physical representation. We must discard models based on the acoustic point of view. Nonlinear energy losses in steep wave fronts and energy flow to the wave structure from combustion must be accommodated. By far the most effective method for incorporating this large array of physical/chemical interactions is by application of the global nonlinear energy balance. Methods based on the usual perturbed acoustic wave equation cannot properly account for the many interactions that must be included. To make the mathematical problem tractable, we choose to avoid fashionable numerical strategies such as method of characteristics or a full CFD treatment of the problem. Either of these techniques would likely represent a handicap in approaching the problem solution we seek here.

There is a vast array of data that prove that the wave motions characterizing the nonlinear instability problem are shock-like rather than simple acoustic waves. A very thorough discussion of the facet of nonlinear instability is given in a companion paper.[50] Thus, whatever is done in modeling nonlinear effects, this feature must play a major role. In Ref. 50 we demonstrate that the natural evolution of an initially linear system composed of superimposed standing acoustic modes will transition to a traveling shock wave if the system in linearly unstable. That is, if the linear growth rate is positive, given sufficient time (sometimes referred to as the delay time[16,17]), the wave system will steepen into a shock if there is enough energy to give nonzero amplitude to one or more of the constituent acoustic modes. This process can be made to occur almost instantaneously if the chamber is pulsed as is often done in motor stability testing.

A. Culick's Nonlinear Model

Building on his linear acoustic wave equation model, Culick has approached the nonlinear instability problem by carrying higher-order terms that represent the coupling between the acoustic modes.[5,21,28]

His nonlinear model traces cascading of energy from lower-order to higher-order modes. Figure 3 shows a frame from an animation of the development of the wave system with time predicted by Culick's model.

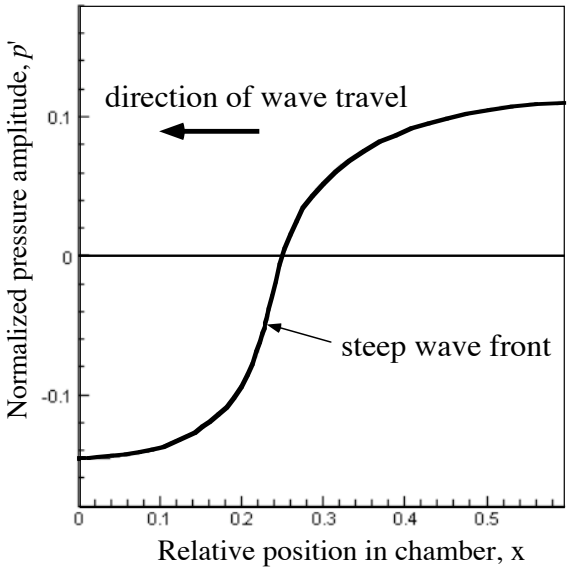

Fig. 3 Culick's fully steepened wave.

At the instant shown, the wave has nearly reached its final limit condition, and the wave front is moving to the left. This wave is the composite of twenty acoustic modes. Energy from the lower order modes has cascaded to the higher modes until the stationary state shown in the figure has been reached. This "mode coupling" effect clearly represents the natural steepening process. What began as a set of standing acoustic modes has transitioned into a single traveling steep-fronted wave. Once limiting has occurred, the wave simply bounces back and forth from one end of the chamber to the other. The period of oscillation corresponds to the first longitudinal acoustic period. What is shown here agrees in every respect with the fully steepened condition described in earlier works by the present writer.[23,24]The calculations and animation from which Fig. 3 was taken were carried out by J. French. He has fully implemented Culick's nonlinear model in the SSP. It can be run for longitudinal modes with arbitrary chamber cross-sectional area.

B. Mathematical Strategy

In the problem of central interest here, we are not concerned with the steepening process, *per se*, rather, we wish to understand the gas motions in the fully steepened state. Figure 4 illustrates several aspects of the problem we must solve. Plots of this sort can be made by application of the model implicit in Eq. (3).

With this information in hand, one must now seek to take best advantage of it. Experiments show that if the system is pulsed or if measurements are taken when it is in a fully steepened state, the acoustic components will display very nearly fixed relative amplitudes. We describe this as the *frozen* state,[23,24] in which it is no longer necessary to account for energy transfer between the modes. A simple model can be used to represent the composite wave system.

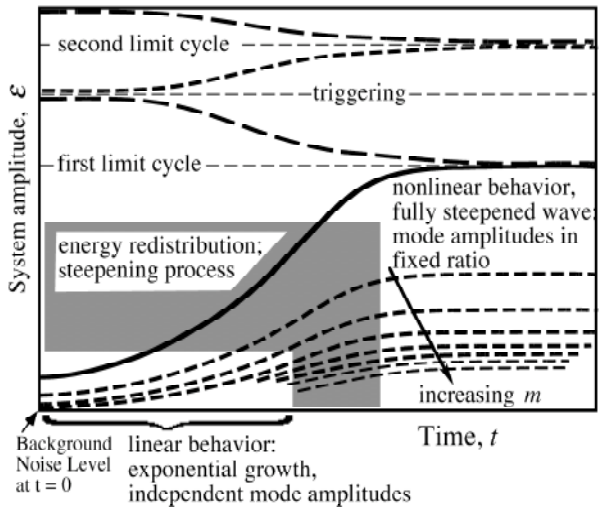

Fig. 4 Nonlinear evolution of system amplitude.

This diagram shows in schematic form all features of combustion instability that appear experimentally. Furthermore, it provides a useful way to categorize the various analytical methods by which we attempt to understand this very complicated physical problem. Figure 6 shows that if the waves grow from noise in the linear fashion, the motion is linear and each acoustic mode grows individually according to the balance of energy gains and losses peculiar to that operating frequency. In general, the lowest order mode grows most rapidly because it requires less energy to excite. As the oscillations grow to finite amplitude, nonlinear effects appear and energy is redistributed from lower to higher modal components; this cascading process is the basis of Culick's nonlinear model.

As the wave steepens, the relative amplitudes of the constituent acoustic modes reach a frozen state corresponding to shock-like behavior. This is the fully nonlinear state illustrated in the figure. In pulse testing of motors, the steepening process is almost instantaneous. For example, Brownlee[16] notes that when the pulse is fired, "… the injected flow disturbance traversed the length of the motor, partially reflected at the nozzle end, and became a steep-fronted shock-like wave in one cycle." Thus, in modeling such effects, it is unnecessary to trace the full steepening process. The relative wave amplitudes are readily estimated from a large database of experimental data. It is readily established that precise knowledge of the relative amplitudes is not necessary to achieve an accurate estimate of the limit cycle and triggering amplitudes.

We must formulate a mathematical strategy that yields the essential information, namely the limit amplitude reached by the system in the fully steepened state. This is the information required by the motor designer in assessing potential vibration levels, and as we will show, the severity of heat loads and force levels on fragile system components.

C. Traveling Shocked Acoustic Waves by Superposition of Standing Normal Modes

A key to simplifying the nonlinear problem is to assume that the *fully steepened traveling* wave is a composite of the chamber normal modes:

$$p^{(1)}(\boldsymbol{r},t) = \varepsilon(t)\sum_{n=1}^{\infty} A_n(t)\psi_n(\boldsymbol{r}) \qquad (9)$$

where $\varepsilon(t)$ is the instantaneous amplitude and n is the mode integer. This is a proven simplifying strategy[23,24] that follows directly as the final form reached in Culick's calculations. It conforms well to all experimental features that must be accommodated in our solution algorithm. Before proceeding with the analysis, let us first test this model in several ways to see if it contains

the necessary features and flexibility. Equation (9) provides a useful tool and a way to avoid all computational difficulties associated with modeling of the unsteady flowfield. In the case of simple longitudinal oscillations in a chamber of constant cross section, the functions in the summation are, for example,

$$\begin{cases} A_n(t) = \left(\dfrac{8n}{4n^2+1}\right)\sin\left(\dfrac{n\pi a_0}{L}\right) \\ \psi_n(r) = \cos\left(\dfrac{n\pi z}{L}\right) \end{cases} \tag{10}$$

where L is the chamber length and z is the axial position. If Eq. (1) is evaluated with these parameters, the waveform illustrated in Fig. 5a is produced. This should be compared to a measured waveform in Fig. 5b. The data shown came from precision pressure measurements in a liquid rocket preburner undergoing high-amplitude nonlinear longitudinal oscillations.

It is clear that Eq. (9) yields an excellent model of the actual waveform. It can be used to represent any experimental waveform by fitting a Fourier series to the data. It is known that once the wave has reached the limit cycle conditions, the waveform remains essentially frozen; only the amplitude then changes with time. This is a truly valuable and very powerful computational simplification.

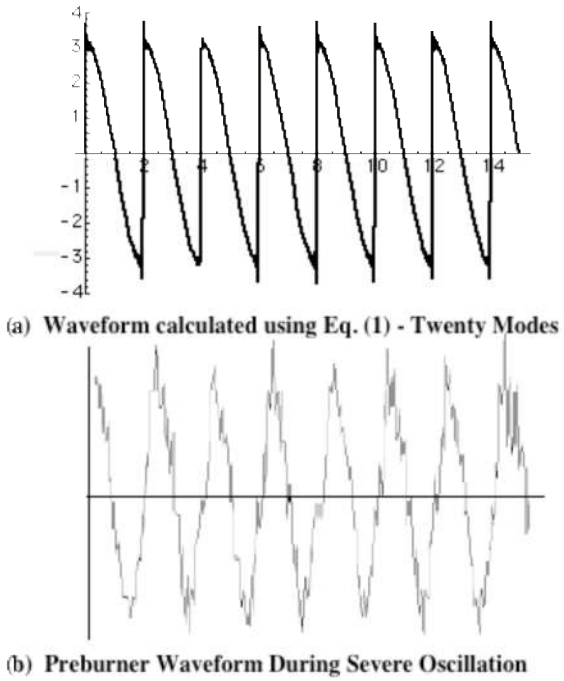

Fig. 5 Measured vs. calculated waveform.

D. Shockwaves in Blomshield's Motor Data

To further test the application of Eq. (9) we can (by using spectral measurements that give each acoustic mode amplitude as a function of frequency) simulate the actual wave motion in the motor test. Figure 6 shows data of this type for a full-star motor with nominal first longitudinal (1L) mode frequency of about 300 Hz.

Note that the relative amplitudes stay fixed for a considerable time period as we have assumed in Eq. (9). Using these amplitudes in Eq. (9) we can examine the wave form of the resulting traveling pressure oscillation. Figure 7 shows such a simulation for the spectrum of Fig. 6. A half-cycle is shown with the traveling wave traveling from left to right. Ten modes were used.

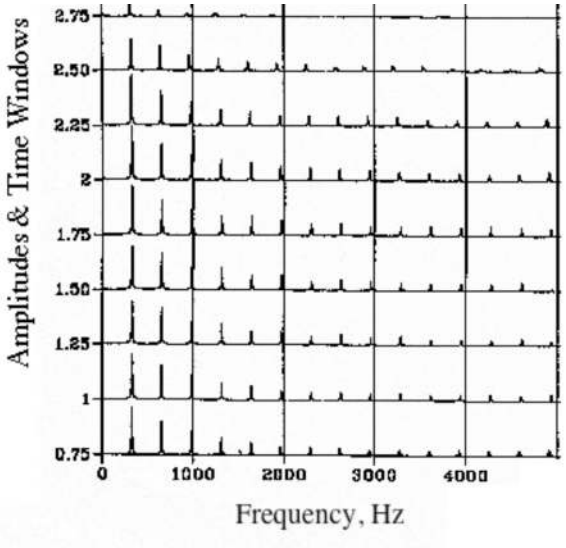

Fig. 6 Nonlinear evolution of system amplitude.

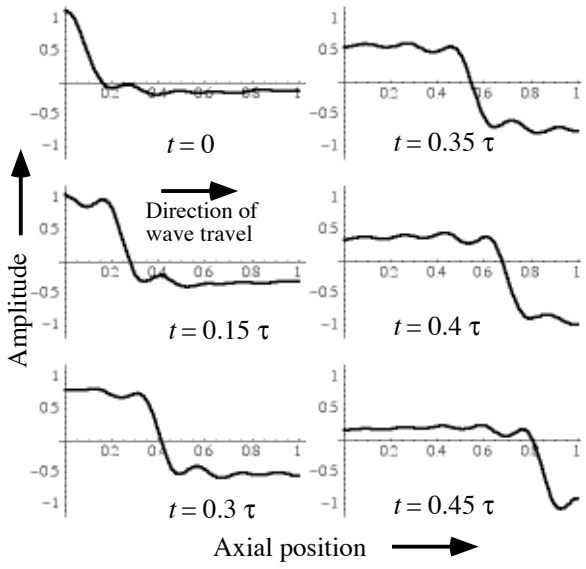

Fig. 7 Shockwave in motor no. 7.[34]

The motion shown in the plot repeats with the steep wave bouncing to and fro from one end to the other. What is shown agrees fully with the final state reached in a typical simulation from Culick's model. The benefit from using Eq. (9) is that a time consuming transition calculation is not needed. A reasonable analytic wave form model of the type shown in Eq. (10) can be used or, as we have demonstrated, actual spectral data measured in the subject burner can be used in representing the nonlinear oscillations.

E. Shockwave Energy Loss

It is now required to examine nonlinear terms arising from the expansion of Eq. (2). The most important of these are the energy losses incurred in steep wave fronts. Let us focus on the set of terms in Eq. (2) that are associated with shock layer effects. The details of the calculation are described in Ref. 50. After temporal and spatial averaging, we are left with

$$\iiint_V \left\langle \frac{\delta^2}{(\gamma-1)Pr}\nabla^2 T + \delta_d^2 \left(\nabla\cdot\boldsymbol{u}\right)^2 \right\rangle \mathrm{d}V \qquad (11)$$

Those readers with training in gasdynamics will recognize in this term the source of the entropy gain and associated energy loss in a steep wave front. In fact, this term is usually ignored because it is only important if there are very steep gradients in particle velocity and temperature. Let us evaluate this term by considering a very small portion of the chamber volume that encompasses the shock layer formed by a steepened wave system as described earlier. The shock layer can be treated as a region of nonuniformity as illustrated in Fig. 8.

Following standard procedures, Eq. (11) can be reduced to the classical textbook result showing the origin of the entropy gain in the shockwave. By manipulations using the Rankine-Hugoniot equations, we find the formula for the energy loss in the steep wave to be

$$\begin{aligned}\left(\frac{dE}{dt}\right)_{\text{shock}} &= -\frac{S_{\text{port}}}{\gamma(\gamma-1)}\frac{(s_2-s_1)^*}{c_v} \\ &= -\left(\frac{\varepsilon_{\text{shock}}}{\bar{P}}\right)^3 S_{\text{port}}\left(\frac{\gamma+1}{12\gamma^3}\right)\end{aligned} \qquad (12)$$

which leads to a simple approximation for the nonlinear stability parameter in Eq. (17), namely

$$\alpha^{(2)} = -\frac{(\gamma+1)}{3E^2}\left(\frac{\xi}{2\gamma}\right)^3 S_{\text{port}} \qquad (13)$$

ξ is a factor dependent upon the assumed waveform for the traveling shock wave, and reference area is the chamber port area at the shock front. In the longitudinal case, this is simply the cross-sectional area of the duct at a convenient location.

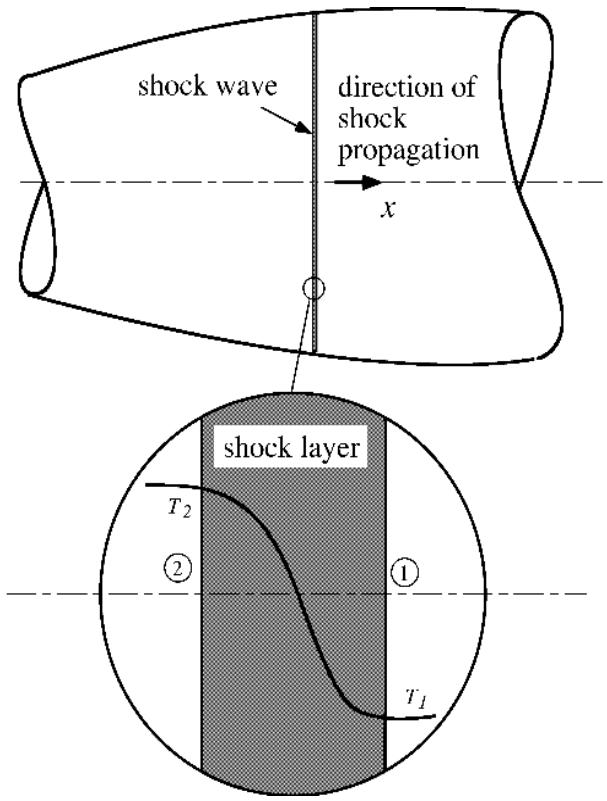

Fig. 8 Shock layer structure.

This nonlinear loss effect is the principal damping mechanism in both liquid and solid propellant motors, and is the key element in understanding the limit cycle behavior so often encountered when finite amplitude waves appear. It is tempting to carry the implied perturbation series in Eq. (3) to orders higher than second in the system amplitude. However, this is not justified in the present situation because we assume that the unsteady flow-field and mode shape information for the chamber are accurate only to the first order in wave amplitude. Let us now test the results we have found against experimental evidence.

F. Limit Cycle Amplitude

A very important goal of the present work is the accurate estimation of the limit amplitude to which oscillations will rise in the course of their growth. Linear theory as in the SSP gives no information in this regard. There is, however, a well-known rule of thumb that suggests that large values of the linear growth rate (estimated for example by using Eq. (7)) correlate with large values of the limit cycle amplitude. Clearly it is the latter amplitude that is of concern, since it is a measure of vibration and other impacts on the system due to the oscillations.

What is required is information concerning the limit amplitude reached as the wave system approaches a fully steepened form. Equation (3) provides the required limit amplitude. In the fully steepened state, the wave amplitude is stationary, and it is readily seen that the limit amplitude is

$$\varepsilon_{\text{limit}} = -\frac{\alpha^{(1)}}{\alpha^{(2)}} \tag{14}$$

This is physically meaningful only when $\alpha^{(2)}$ is negative. This will *always* be the case for the shock loss mechanism described by Eq. (13). To the knowledge of the authors, there has never been either experimental or theoretical evidence of second order interactions that are not damping effects. However, there may be nonlinear driving mechanisms yet to be discovered. Equation (14) has been tested for many solid rocket data sets and has been found to yield an excellent estimate of the limit amplitude. Again, note that good results depend critically on a valid linear stability estimate.

Jensen and Beckstead successfully used the equivalent of Eq. (14) in developing their well-known Pi Theorem.[23,33] This correlation allowed improved data reduction for T-burner tests, thus yielding far better response function values than can be secured by the usual blind application of the SSP algorithm. Why this promising approach was not adopted more generally remains a mystery.

G. Triggering Amplitude

This is a controversial subject. If one examines Fig. 4, in the context of Eq. (3) extended to fourth order in the wave amplitude, it is apparent that it is theoretically possible to raise the amplitude of a system oscillating in its lowest limit cycle to a yet higher limit amplitude by adding sufficient energy in a strong pulse. This is what might be termed *true triggering*. Careful examination of solid rocket data has convinced the authors that this scenario seldom fits what is actually observed. In every case, motors that exhibit "triggering" are *linearly unstable* motors. That is, they are not stable motors that are *triggered* into a high-amplitude limit cycle. When such burners operate without deliberate pulsing, the wave system grows so slowly from the always-present random noise, that oscillations are often barely measurable by the end of the burn. However, when the motor is disturbed by a sufficiently large pulse, the broadband energy increment can excite finite amplitude steep-fronted waves. The system then grows rapidly to the limit cycle amplitude. Calculations using Eq. (3) agree very well with actual observations. We believe that true triggering is seldom, if ever, observed in actual rocket motors. Much of the confusion over this issue has resulted from application of faulty analytical codes that almost always predict a linearly stable system. A classic example can be found in the Blomshield data.[34] Every motor fired in this test series was predicted by the SSP to be linearly stable. In fact there is no doubt that many of the motors were linearly unstable at least during part of the firing. Unless pulsed, only very low level oscillations were present. Sufficiently strong pulsing during linearly unstable operation led to violent oscillations in several tests.

These observations help us to understand the seemingly contradictory and nearly inexplicable information depicted in Fig. 1. When confronted by such data, many experimentalists tend to explain the scatter and obvious departure from expected behavior (usually based on incorrect use of SSP data reduction) by invoking errors or uncertainties in the T-burner data needed in the SSP evaluations. As already pointed out, there is cause to worry about the response function data itself; it is usually determined by applying the SSP to the raw T-burner data. We see here a classical case of the compounding of errors.

IV. The DC Pressure Shift

The mean pressure rise, or DC shift, is an oft-observed feature of nonlinear instability. It is obviously closely coupled to the growth and limiting of the system of acoustic waves. A test of the validity of the theory presented in this paper is its ability to predict this important classical feature of combustion instability. What we will demonstrate here is that the same mechanism, pressure coupling, that drives the oscillations (first term in Eq. (7)) is also the source of the DC shift phenomenon.

Until now, explaining the mean pressure excursion required invoking *ad hoc* velocity coupling or "acoustic erosivity" effects.[53] These confusing and often simply misleading paraphernalia can now be discarded.

Clearly, any attempt to understand one nonlinear feature without due attention to other closely connected features does not take full advantage of the experimental data. In this section we demonstrate the benefits of accommodating all of the observations in formulating the mathematical approach.

Previous theoretical models have been based on the assumption that the mean gas properties remain constant. For example, Culick writes: "…we assume that the average values do not vary with time. That is not an essential assumption, but to correct it requires considerable elaboration not justified here. However, there are practical situations in which changes in the average values, particularly the pressure, are important. No thorough analysis of such cases has been given."[8] In what follows we present the missing analysis.

The formulation described in the last section has been deliberately written without the assumption of constant mean properties. Thus we are able to study the cou-

pling between the unsteady and *quasi-steady* gas motions. It is assumed that the chamber mean temperature is controlled by combustion heat release and is therefore essentially constant. Then the state equation shows that mean pressure and density are slowly changing functions of time. The surface reference Mach number and the wave amplitude are also slow functions of time as already demonstrated.

A. Formula for Rate of Change of Mean Pressure

The source of the DC shift is readily found if nonlinear terms are retained in the continuity equation. Expanding Eq. (6) and taking the time average yields

$$\frac{\mathrm{d}\bar{P}}{\mathrm{d}t} = -\nabla\cdot\left(\bar{M}_b\bar{\rho}\boldsymbol{U}\right) - \frac{\varepsilon^2}{\gamma}\nabla\cdot\left\langle p'\boldsymbol{u}'\right\rangle \tag{15}$$

where the first term on the right represents quasi-steady mass flux at the chamber boundaries due to combustion and nozzle outflow. The similarity of the second term to the pressure-coupled acoustic driving in Eq. (21) is intriguing. Integration over the chamber volume leads to the equation for the rate of change of the quasi-steady chamber operating pressure:

$$\frac{\mathrm{d}\bar{P}}{\mathrm{d}t} = \left\{\begin{array}{l} -\dfrac{1}{\bar{V}}\displaystyle\iint_S \boldsymbol{n}\cdot\left(\bar{\rho}\bar{M}_b\boldsymbol{U}\right)\mathrm{d}S - \\ -\varepsilon^2\left(\dfrac{1}{\gamma\bar{V}}\right)\displaystyle\iint_S \boldsymbol{n}\cdot\left\langle p'\boldsymbol{u}'\right\rangle\mathrm{d}S \end{array}\right\} \tag{16}$$

The first term is handled by means of the standard steady internal ballistics calculations; the second leads to the mean pressure shift. Notice that it is proportional to the second order in the wave amplitude. Equation (16) confirms the anticipated coupling between the mean pressure rise and the growth and limiting of the pressure oscillations.

B. Simulating and Predicting Motor Behavior

The results for the nonlinear system growth and the corresponding mean pressure excursion must be computed simultaneously. When the several system models are collected and the integrals are performed, we are left with a pair of coupled nonlinear, ordinary differential equations:

$$\left\{\begin{array}{l} \dfrac{\mathrm{d}\varepsilon}{\mathrm{d}t} = \alpha^{(1)}\varepsilon + \alpha^{(2)}\varepsilon^2 + \cdots \\ \dfrac{\mathrm{d}\bar{P}}{\mathrm{d}t} = \beta^{(1)} + \beta^{(1)}\varepsilon^2 \end{array}\right. \tag{17}$$

These are readily solved using a simple numerical algorithm. The result is the time history of the growth and limiting of the pressure oscillation amplitude and the accompanying growth and limiting of the mean pressure amplitude. These results agree in every way with motor data.

C. Response Function from the DC Shift

A test of the validity of any new theory is its ability to predict new information not available in the theory that it is intended to replace. We will briefly demonstrate that the new nonlinear combustion instability theory passes this test.

Consider a case in which the limit amplitude has been reached and the mean pressure is no longer growing. We will demonstrate in the next section using experimental data that the rapid growth of both mean and fluctuating pressure cease at very nearly the same time. At this condition, the rate of change of pressure is zero, and Eq. (16) can be evaluated. One finds

$$0 = \left[\begin{array}{l} \beta c\dfrac{\left(P_0\bar{P}\right)^n}{a_0}S_b - \\ \bar{P}\left(\dfrac{2}{\gamma+1}\right)^{\frac{(\gamma+1)}{2(\gamma-1)}}S_{\text{Throat}} \end{array}\right] - \frac{\varepsilon^2}{\gamma}\iint_S \boldsymbol{n}\cdot\left\langle p'\boldsymbol{u}'\right\rangle\mathrm{d}S \tag{18}$$

where the terms in the square brackets represent the classical solid motor internal ballistics. The last term is clearly related to the admittance function for the propellant. Write, for example, for normal wave incidence

$$\boldsymbol{n}\cdot\left\langle p'\boldsymbol{u}'\right\rangle = -\frac{\bar{M}_b}{\gamma}A_b^{(r)}\left\langle p'^2\right\rangle \tag{19}$$

Then we can solve for the admittance value for a given wave geometry and measured pressure shift. After several lines of algebra we find that

$$\frac{P_{\text{lim}}}{P_{\text{std}}} = \left[1 + \frac{\varepsilon^2 C_2}{4\gamma^2}\left(A_b^{(r)} + C_1\right)\right]^{\left(\frac{1}{1-n}\right)} \tag{20}$$

where n is the burning rate exponent. The pressure ratio on the left-hand side is the ratio of the measure mean pressure shift to the expected mean pressure when no instability is present. This is easily calculated using the SPP or other internal ballistics codes. The two parameters shown are

$$C_1 = \begin{cases} 0 & \text{waves normal to surface} \\ 1 & \text{waves parallel to surface} \end{cases} \tag{21}$$

which accounts for the velocity coupling when waves are parallel to the surface. Also one must know

$$C_2 = \frac{1}{S_b}\iint_S \psi^2\left(\boldsymbol{r}\right)\mathrm{d}S \tag{22}$$

which accounts for the effective mode shape of the wave. For the case of longitudinal oscillations, this coefficient is approximately 0.5.

Assuming that the wave limit amplitude and mean pressure have been measured, then one can solve Eq. (20) to find the admittance function.

For example, for motor 3 in Blomshield's data set we find that

$$\left(A_b^{(r)}+1\right)=\left(\frac{2\gamma}{\varepsilon}\right)^2\left[\left(\frac{P_{\lim}}{P_{\text{std}}}\right)^{(1-n)}-1\right] \qquad (23)$$

Inserting measured quantities yields an admittance value of approximately

$$A_b^{(r)}=4$$

This agrees reasonably well with T-burner measurements. This approach will require considerable refinement, but it may eventually lead to improved experimental techniques for characterizing the propellant response function.

V. Results

The methods described here are being used to enhance the SSP. This will enable the rocket analyst/designer to predict the stability of a given system and to diagnose sets of experimental data.

We show here some preliminary results from application of Eqs. (17) to Blomshield's data set.[34-36,54,55] In virtually all of his motor configurations, the standard stability prediction code predicted stable behavior as depicted in Fig. 1. Yet, many of the motors were readily pulsed into high-amplitude oscillations. We wish to understand this apparent triggering phenomenon. Numerical solutions of Eq. (17) provide the required information.

Figure 9 shows a pressure vs. time trace for a cylindrical motor from this test series.

The mean pressure shift and pressure oscillations are clearly shown. Data came from a pressure transducer at the motor forward end. This motor exhibited a spectrum dominated by the 1L (first longitudinal mode) accompanied by a great many harmonics representing strong evidence for steep-fronted waves as already described. The progressive pressure rise results from the increasing burning surface area with time.

Figure 10 shows the predicted behavior of this motor found by solving Eqs. (32) using geometrical and physical data from the tests; no curve fitting was employed.

All key attributes of the actual data are well represented. Notice that even though the system is linearly unstable, no wave growth or DC shift occurs unless the motor is pulsed. Examination of the numerical results shows that this motor was marginally stable during the first part of the burn, but the net linear growth rate became positive after about t = 0.5 sec. The motor was then susceptible to pulsing, and could be "triggered" into violent oscillations. Parametric studies have shown that the predicted DC shift and corresponding oscillation limit cycle amplitude are insensitive to the pulse amplitude; this agrees with experimental findings.

Similar comparisons of predicted and measured behavior are shown in Figs. 11-14 for the other two cylindrical motors (10 and 13) fired in this test series. Motor 10 follows closely the pattern that was predicted for motor 9. Both of these were full-length motors with oscillation frequency of about 300 Hz. Motor 13 was a half-length motor with otherwise similar geometry.

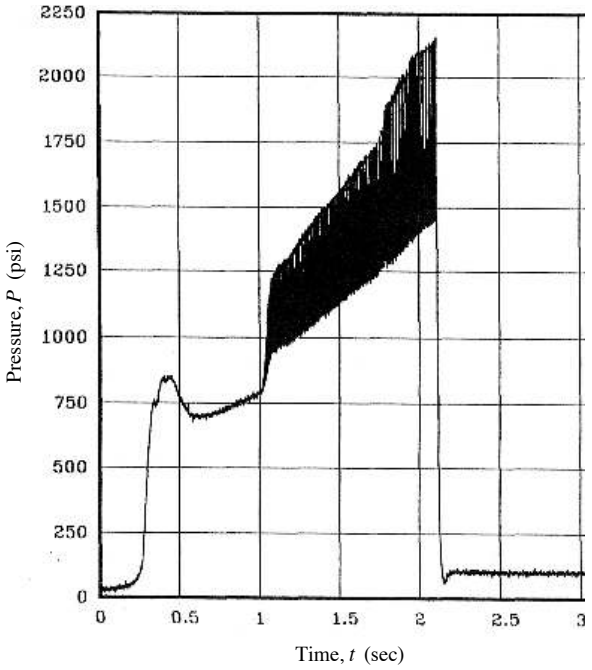

Fig. 9 Pressure vs. time for motor no. 9.[34]

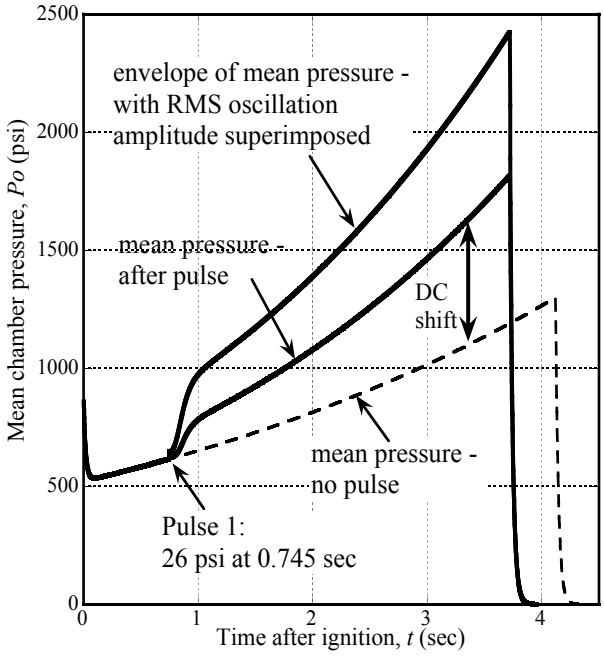

Fig. 10 Simulation of motor no. 9.[56,57]

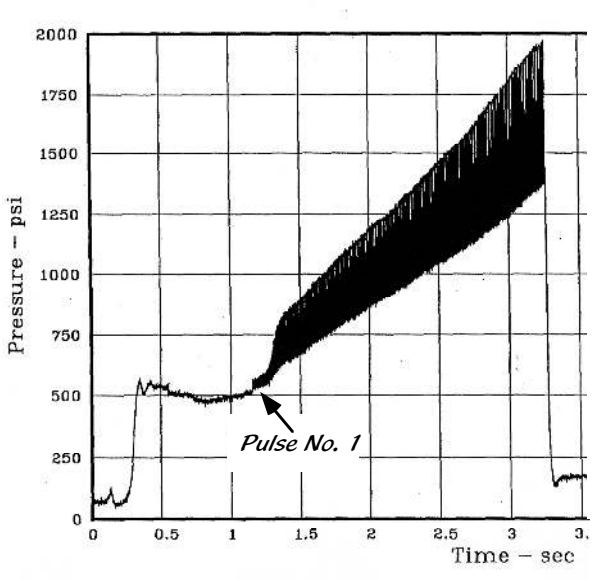

Fig. 11 Pressure vs. time for motor no. 10.[34]

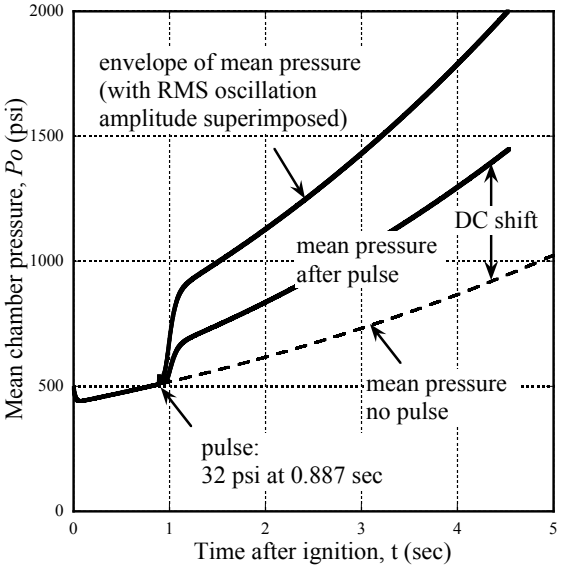

Fig. 13 Simulation of motor no. 10.[34]

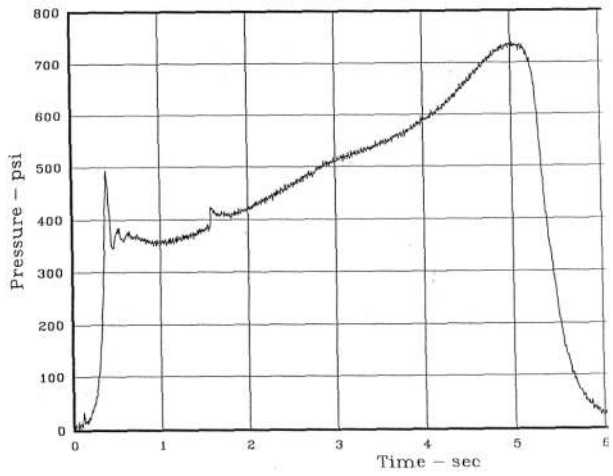

Fig. 12 Pressure vs. time for motor no. 13.[34]

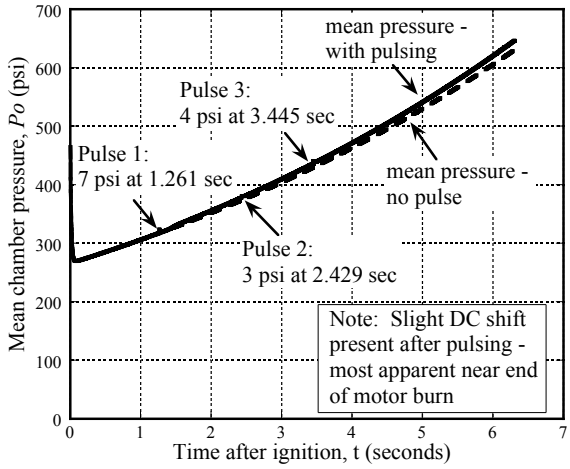

Fig. 14 Simulation of motor no. 13.[34]

Motors 11 and 13 had nozzles sized to yield an average operating pressure of 500 psi; Motor 9 was intended to operate at about 1000 psi.

All motors described here were predicted to be stable throughout the firing by the SSP. Again, we see evidence of the failure of this analytical tool.

Note that in both full length motors our new predictive computer code has captured all of the main features shown in the experimental data.

In the half-length motor (13) we see some interesting results. This motor was pulsed three times and did not exhibit the violent oscillations observed in the other two tests. However, careful inspection of the data reveals that oscillations were indeed present despite the prediction from the SSP code that motor 13 was a stable motor. Since a large DC shift did not appear, the authors of Ref. (34) expressed their belief that this was indeed a stable firing in agreement with the SSP prediction. If the reader will examine the last part of the pressure time trace evidence of a DC shift is clearly present. It apparently grew without a pulse from pressure oscillations already in the system.

For motor. 13 the new predictive algorithm yields a result that is in good agreement with the measurements. No violent DC pressure rise was predicted, but, again, a small elevation was present as in the experimental data. We must conclude that motor 13 was indeed unstable! The main reason for the less violent oscillations was the reduced propellant surface area in the half-length grain. The primary energy source for both the oscillations and

the DC pressure rise was thereby much reduced. Thus, on the basis of a limited number of test cases we feel that the basic validity of our approach has been demonstrated.

To summarize: we have devised a new procedure for estimating the tendency for a given rocket motor configuration to exhibit nonlinear combustion instability. The new algorithm gives not only growth rate information and the associated stability maps, but more importantly predicts the evolution of the system oscillation amplitude and the mean pressure shift. These analytical/numerical tools promise to give the motor designer the ability to avoid design features that may promote combustion instability much earlier in the development cycle than possible using other methods.

If combustion instability problems are encountered in the motor test phase of development, these new tools yield an improved method for correlating experimental data and correctly interpreting the results. They also provide the ability to test and perfect corrective mechanisms if these become necessary.

VI. Concluding Remarks

In this paper we have demonstrated a predictive algorithm based on sound theoretical foundations that fully explains the nonlinear behavior observed in unstable rocket motor systems. The close connection between pressure coupling, the main linear driving mechanism in combustion instability, and the DC pressure shift has been demonstrated. Knowledge of the physical parameters that control the pressure coupling, namely the admittance function or response function of the propellant, makes it possible to determine the growth and limiting amplitude of both the wave system and the accompanying mean pressure shift.

This research has been conducted from the outset with the intention that it be used in constructing an improved version of the Standard Stability Prediction code.

Much work is left in refining the new computational technique. Eventually these tools will be available in a practical form and with a powerful user interface to enable the rocket motor engineer to better deal with combustion instability problems.

Acknowledgements

This work was sponsored partly by the University of Tennessee, UTSI, and partly by Software and Engineering Associates, Inc., SEA, Carson City, NV. Dr. J. C. French was the program manager. The first author wishes to express appreciation for additional support from the Edward J. and Carolyn P. Boling Chair of Excellence in Advanced Propulsion, University of Tennessee.

References

[1]Cheng, S. I., "High Frequency Combustion Instability in Solid Propellant Rockets (Parts I and Ii)," *Jet Propulsion,* Vol. 24, No. 1, 1954, pp. 27-32, 102-109.

[2]Culick, F. E. C., "Acoustic Oscillations in Solid Propellant Rocket Chambers," *Acta Astronautica,* Vol. 12, No. 2, 1966, pp. 113-126.

[3]Culick, F. E. C., "The Stability of One-Dimensional Motions in a Rocket Motor," *Combustion Science and Technology,* Vol. 7, No. 4, 1973, pp. 165-175.

[4]Culick, F. E. C., "Stability of Three-Dimensional Motions in a Rocket Motor," *Combustion Science and Technology,* Vol. 10, No. 3, 1974, pp. 109-124.

[5]Culick, F. E. C., "Nonlinear Behavior of Acoustic Waves in Combustion Chambers," California Institute of Technology, Pasadena, CA, 1975.

[6]Culick, F. E. C., "Nonlinear Behavior Acoustic Waves in Combustion Chambers, Parts 1 and 2," *Acta Astronautica,* Vol. 3, 1976, pp. 714-757.

[7]Culick, F. E. C., "Combustion Instabilities in Propulsion Systems," *American Society of Mechanical Engineers, Noise Control and Acoustics Division,* Vol. 4, 1989, pp. 33-52.

[8]Culick, F. E. C., and Yang, V., "Prediction of the Stability of Unsteady Motions in Solid Propellant Rocket Motors," *Nonsteady Burning and Combustion Stability of Solid Propellants*, Vol. 143, edited by L. De Luca, E. W. Price, and M. Summerfield, AIAA Progress in Astronautics and Aeronautics, Washington, DC, 1992, pp. 719-779.

[9]Hart, R. W., and McClure, F. T., "Combustion Instability: Acoustic Interaction with a Burning Propellant Surface," *The Journal of Chemical Physics,* Vol. 10, No. 6, 1959, pp. 1501-1514.

[10]Hart, R. W., and McClure, F. T., "Theory of Acoustic Instability in Solid Propellant Rocket Combustion," *Tenth Symposium (International) on Combustion*, 1964, pp. 1047-1066.

[11]Culick, F. E. C., "Stability of Longitudinal Oscillations with Pressure and Velocity Coupling in a Solid Propellant Rocket," *Combustion Science and Technology,* Vol. 2, No. 4, 1970, pp. 179-201.

[12]Culick, F. E. C., "Combustion Instabilities in Propulsion Systems," *Unsteady Combustion*, Kluwer Academic Publishers, 1996, pp. 173-241.

[13]Price, E. W., and Flandro, G. A., "Combustion Instability in Solid Rockets," AFOSR, Technical Rept. TR-87-0459, February 1987.

[14]Price, E. W. and Sofferis, J. W., "Combustion Instability in Solid Propellant Rocket Motors," *Jet Propulsion,* Vol. 28, 1958, pp. 190-192.

[15]Yang, V., Wicker, J., and Yoon, M. W., "Acoustic Waves in Combustion Chambers," *Liquid Rocket Engine Combustion Instability*, Vol. 169, edited by V. Yang and W. E. Anderson, AIAA Progress in Astronautics and Aeronautics, 1995, pp. 357-376.

[16]Brownlee, W. G., "Nonlinear Axial Combustion Instability in Solid Propellant Motors," *AIAA Journal,* Vol. 2, No. 2, 1964, pp. 275-284.

[17]Brownlee, W. G., "An Experimental Investigation of Unstable Combustion in Solid Propellant Rocket Motors," Ph.D. Dissertation, California Institute of Technology, 1959.

[18]Green, J., L, "Observations on the Irregular Reaction of Solid Propellant Charges," *Jet Propulsion,* Vol. 26, 1956, pp. 655-659.

[19]Nickerson, G. R., Coats, D. E., Hersmen, R. L., and Lamberty, J., "A Computer Program for the Prediction of Solid Propellant Rocket Motor Performance (SPP)," Software and Engineering Associates, Inc., AFRPL TR-83-036, CA, September 1983.

[20]Nickerson, G. R., Culick, F. E. C., and Dang, L. G., "Standardized Stability Prediction Method for Solid Rocket Motors Axial Mode Computer Program," Software and Engineering Associates, Inc., AFRPL TR-83-017, September 1983.

[21]Culick, F. E. C., "Non-Linear Growth and Limiting Amplitude of Acoustic Oscillations in Combustion Chambers," *Combustion Science and Technology,* Vol. 3, No. 1, 1971, pp. 1-16.

[22]Culick, F. E. C., "Combustion Instabilities: Mating Dance of Chemical, Combustion, and Combustor Dynamics," AIAA Paper 2000-3178, July 2000.

[23]Flandro, G. A., "Approximate Analysis of Nonlinear Instability with Shock Waves," AIAA Paper 82-1220, July 1982.

[24]Flandro, G. A., "Energy Balance Analysis of Nonlinear Combustion Instability," *Journal of Propulsion and Power,* Vol. 1, No. 3, 1985, pp. 210-221.

[25]Flandro, G. A., "Analysis of Nonlinear Combustion Instability," SIAM Minisymposium, March 1998.

[26]Yang, V., Kim, S. I., and Culick, F. E. C., "Triggering of Longitudinal Pressure Oscillations in Combustion Chambers, I: Nonlinear Gasdynamics," *Combustion Science and Technology,* Vol. 72, No. 5, 1990, pp. 183-214.

[27]Culick, F. E. C., "Some Recent Results for Nonlinear Acoustics in Combustion Chambers," *AIAA Journal,* Vol. 32, No. 1, 1994, pp. 146-168.

[28]Culick, F. E. C., Burnley, V. S., and Swenson, G., "Pulsed Instabilities in Solid-Propellant Rockets," *Journal of Propulsion and Power,* Vol. 11, No. 4, 1995, pp. 657-665.

[29]Levine, J. N., and Baum, J. D., "A Numerical Study of Nonlinear Phenomena in Solid Rocket Motors," *AIAA Journal,* Vol. 21, No. 4, 1983, pp. 557-564.

[30]Brownlee, W. G. a. K., G H, "Shock Propagation in Solid-Propellant Rocket Combustors," *AIAA,* Vol. 4, No. 6, 1966, pp. 1132-1134.

[31]Malhotra, S. and Flandro, G. A, "On the Origin of the Dc Shift," AIAA Paper 97-3249, July 1997.

[32]Price, E. W., "Experimental Observations of Combustion Instability," *Fundamentals of Solid-Propellant Combustion*, Vol. 90, edited by K. Kuo and M. Summerfield, AIAA Progress in Astronautics and Aeronautics, New York, 1984, pp. 733-790.

[33]Jensen, R. C., and Beckstead, M. W., "Limiting Amplitude Analysis," Hercules Incorporated, Magna, Utah, 1973.

[34]Blomshield, F. S., "Stability Testing and Pulsing of Full Scale Tactical Motors, Parts I and II," Naval Air Warfare Center, NAWCWPNS TP 8060, February 1996.

[35]Blomshield, F. S., Crump, J. E., Mathes, H. B., Stalnaker, R. A., and Beckstead, M. W., "Stability Testing of Full-Scale Tactical Motors," *Journal of Propulsion and Power,* Vol. 13, No. 3, 1997, pp. 349-355.

[36]Blomshield, F. S., Mathes, H. B., Crump, J. E., Beiter, C. A., and Beckstead, M. W., "Nonlinear Stability Testing of Full-Scale Tactical Motors," *Journal of Propulsion and Power,* Vol. 13, No. 3, 1997, pp. 356-366.

[37]Culick, F. E. C., "Rotational Axisymmetric Mean Flow and Damping of Acoustic Waves in a Solid Propellant Rocket," *AIAA Journal,* Vol. 4, No. 8, 1966, pp. 1462-1464.

[38]Culick, F. E. C., "Remarks on Entropy Production in the One-Dimensional Approximation to Unsteady Flow in Combustion Chambers," *Combustion Science and Technology,* Vol. 15, No. 4, 1977, pp. 93-97.

[39]Culick, F. E. C., "A Note on Rayleigh's Criterion," *Combustion Science and Technology,* Vol. 56, 1987, pp. 159.

[40]Culick, F. E. C., "Rotational Axisymmetric Mean Flow and Damping of Acoustic Waves in a Solid Propellant Rocket," *Journal of Propulsion and Power,* Vol. 5, No. 6, 1989, pp. 657-664.

[41]Culick, F. E. C., Lin, W. H., Jahnke, C. C., and Sterling, J. D., "Modeling for Active Control of Combustion and Thermally Driven Oscillations," *Proceedings of the American Control Conference. Published by American Automatic Control Council, Green Valley, AZ, USA,* Vol. 7, 1991, pp. 2939-2948.

[42]Lovine, R. L., Dudley, D. P., and Waugh, R. D., "Standardized Stability Prediction Method for Solid Rocket Motors," Aerojet Solid Propulsion Co., Vols. I, II, III Rept. AFRPL TR 76-32, CA, May 1976.

[43]Flandro, G. A., "Effects of Vorticity Transport on Axial Acoustic Waves in a Solid Propellant Rocket Chamber," *Combustion Instabilities Driven by Thermo-Chemical Acoustic Sources*, Vol. NCA 4, HTD 128, American Society of Mechanical Engineers, New York, 1989, pp. 53-61.

[44]Flandro, G. A., "Effects of Vorticity on Rocket Combustion Stability," *Journal of Propulsion and Power,* Vol. 11, No. 4, 1995, pp. 607-625.

[45]Flandro, G. A., "On Flow Turning," AIAA Paper 95-2530, July 1995.

[46]Flandro, G. A., and Majdalani, J., "Aeroacoustic Instability in Rockets," *AIAA Journal,* Vol. 41, No. 3, 2003, pp. 485-497.

[47]Flandro, G. A., and Roach, R. L., "Effects of Vorticity Production on Acoustic Waves in a Solid Propellant Rocket," Air Force Office of Scientific Research, AFOSR Final Rept. 2060 FR, Bolling AFB, DC, October 1992.

[48]Flandro, G. A., and Majdalani, J., "Aeroacoustic Instability in Rockets," AIAA Paper 2001-3868, July 2001.

[49]McClure, F. T., Bird, J. F., and Hart, R. W., "Erosion Mechanism for Nonlinear Instability in the Axial Modes of Solid Propellant Rocket Motors," *ARS Journal,* Vol. 32, No. 3, 1962, pp. 374-378.

[50]Flandro, G. A., Majdalani, J., and French, J. C., "Nonlinear Rocket Motor Stability Prediction: Limit Amplitude, Triggering, and Mean Pressure Shift," AIAA Paper 2004-4054, July 2004.

[51]Malhotra, S., "On Combustion Instability in Solid Rocket Motors," Dissertation, California Institute of Technology, 2004.

[52]Van Moorhem, W. K., "An Investigation of the Origin of the Flow Turning Effect in Combustion Instability," 17th JANNAF Combustion Conference, September 1980.

[53]Levine, J. N. a. B., J. D., "A Numerical Study of Nonlinear Instability Phenomena in Solid Rocket Motors," *AIAA Journal,* Vol. 21, No. 4, 1983, pp. 557-564.

[54]Blomshield, F. S., Bicker, C. J., and Stalnaker, R. A., "High Pressure Pulsed Motor Firing Combustion Instability Investigations," *Proceedings of the 1996 Jannaf 33rd Combustion Meeting*, Naval Postgraduate School, Monterey, CA, 1996.

[55]Blomshield, F. S., and Mathes, H. B., "Pressure Oscillations in Post-Challenger Space Shuttle Redesigned Solid Rocket Motors," *Journal of Propulsion and Power,* Vol. 9, No. 2, 1993, pp. 217-221.

[56]Flandro, G. A., Majdalani, J, and French, J., "Nonlinear Rocket Motor Stability Prediction: Limit Amplitude, Triggering, and Mean Pressure Shift," AIAA Paper 2004-4054, 2004.

[57]Flandro, G. A., Majdalani, J, and French, J., "Incorporation of Nonlinear Capabilities in the Standard Stability Prediction Program," AIAA Paper 2004-4182, 2004.